Society For Biomaterials

Characterization and *in vivo* evaluation of laser sintered dental endosseous implants in dogs

Lukasz Witek,[1] Charles Marin,[2] Rodrigo Granato,[2] Estevam A. Bonfante,[2] Felipe Campos,[3] Julio Bisinotto,[3] Marcelo Suzuki,[4] Paulo G. Coelho[1,5]

[1]Department of Biomaterials and Biomimetics, New York University, New York, New York
[2]Postgraduate Program in Dentistry, UNIGRANRIO University - School of Health Sciences, Duque de Caxias, RJ, Brazil
[3]Department of Oral and Maxillofacial Surgery, Universidade Federal de Uberlandia, Uberlandia, MG, Brazil
[4]Department of Prosthodontics, Tufts University School of Dental Medicine, Boston, Massachusetts
[5]Department of Periodontology and Implant Dentistry, Director for Research, New York University College of Dentistry, New York, New York

Received 28 October 2011; revised 25 March 2012; accepted 31 March 2012
Published online 12 June 2012 in Wiley Online Library (wileyonlinelibrary.com). DOI: 10.1002/jbm.b.32725

Abstract: Laser metal sintering has shown promising results, but no comparison with other commercially available surface has been performed. This study sought to evaluate the biomechanical and histological early bone response to laser sintered implants relative to alumina-blasted/acid-etched (AB/AE). Surface topography was characterized by scanning electron microscopy and optical interferometry. Surface chemistry was assessed by x-ray photoelectron spectroscopy. Beagle dogs ($n = 18$) received 4 Ti-6Al-4V implants (one per surface) in each radius, remaining for 1, 3, and 6 weeks ($n = 6$ dogs per evaluation time) *in vivo*. Bone-to-implant contact (BIC) and bone area fraction occupancy (BAFO) were evaluated. Biomechanical evaluation comprised torque-to-interface failure. The laser sintered surface presented higher S_a and S_q than AB/AE. Chemistry assessment showed the alloy metallic components along with adsorbed carbon species. Significantly higher torque was observed at 1 ($p < 0.02$) and 6 week ($p < 0.02$) for the laser sintered, whereas at 3 week no significant differences were observed. Significantly higher BIC and BAFO was observed for the Laser Sintered ($p < 0.04$, and $p < 0.03$, respectively) only at 1 week, whereas no significant differences were observed at 3 and 6 weeks. The laser sintered implants presented biocompatible and osseoconductive properties and improved biomechanical response compared with the AB/AE surface only at 1 and 6 weeks *in vivo*. © 2012 Wiley Periodicals, Inc. J Biomed Mater Res Part B: Appl Biomater 100B: 1566–1573, 2012.

Key Words: dental implant, biomechanical, laser, histology

How to cite this article: Witek L, Marin C, Granato R, Bonfante EA, Campos F, Bisinotto J, Suzuki M, Coelho PG. 2012. Characterization and *in vivo* evaluation of laser sintered dental endosseous implants in dogs. J Biomed Mater Res Part B 2012:100B:1566–1573.

INTRODUCTION

Research trends have emphasized toward implant design modifications capable of improving the early host implant tissue response[1] and therefore hastening healing time. The main benefit would be the potential reduction in treatment time frames through prosthetic restorations that could be placed in occlusal function earlier than originally recommended protocols.[1–3]

Among implant design modifications attempting to improve the host-to-implant response, implant surface modifications have been extensively investigated.[1–6] The rationale for surface modification lies upon the fact that it is the first part of the implant to interact with biofluids, which potentially alters the cascade of events that leads to bone healing and intimate apposition with the device.[7] Several reviews cover the large number of possibilities included in implant surface modifications, and it is a general consensus that both rough surfaces (over smooth turned surfaces) and surface chemistry (additions of Ca-P–based bioceramics in various forms over noncoated surfaces) may favor the early host-to-implant response.[1,5,6,8]

Whereas implant surface texturing is usually accomplished after the implant device is milled to its desired stock shape, surface roughness may be tailored by its fabrication method such as in laser metal sintering.[9] The process is based on rapid prototyping, where the constructed CAD file is built by a metal forming procedure with a high-power laser beam focused on a metal powder bed and programmed to fuse particles creating a thin metal layer. The process continues until the apposition of layers results in the final shape of the 3D projected device.[10,11] The resulting surface is porous with functionally graded structures where a gradient of porosity is observed perpendicular to the long axis, high porosity at the surface and the constituting core material that may be selected to suit the device's intended use. In addition, a repeated porous pattern with

Correspondence to: E. A. Bonfante; e-mail: estevamab@gmail.com

interconnected pore network has been described after the laser sintering process,[12] potentially improving osseointegration.[13] Since the graded structure decreases the discrepancy between the elastic modulus of titanium and that of surrounding bone, a desirable reduction in the interface stress has also been claimed.[11]

The laser sintering process has a wide range of applications for producing temporary or permanent implantable devices, especially when a design is needed to provide an implant's proper structural and biological function.[14] Although the existing *in vitro*[12] and *in vivo* data[9,15] on laser metal sintering shows promising results, qualitative and quantitative histological comparisons with other commercially available implant surfaces along with biomechanical testing is yet to be understood. Thus, the present study biomechanically (torque-to-interface failure) and histomorphometrically evaluated the effect of laser sintering compared to alumina-blasted/acid-etched implant (AB/AE) surface modifications in the early bone response in a beagle model. We have hypothesized that the intricate surface topography resulting from laser sintering would improve early biomechanical and histomorphometric parameters compared with an AB/AE implant surface.

MATERIALS AND METHODS

The implants used in this study were Ti-6Al-4V screw type implants with 3.75 mm of diameter and 10 mm in length provided by the manufacturer (AB-Dental, Nir Galim, Israel). A total of 86 implants were used and divided in two groups according to surface treatment: Laser Sintered (experimental) and Alumina-Blasted/Acid-Etched (AB/AE) (control) ($n = 38$ per group). The remaining implants ($n = 10$) were used for surface characterization. Specific detail regarding the processing parameters of the surfaces was not provided from the manufacturer. It has been suggested that while high throughput fabrication may be achieved, all dimensional tolerances must be observed during the post fabrication steps, as well as the potential void inclusion during the sintering process.[11]

Surface characterization

The surface characterization was accomplished utilizing three different methods. First, scanning electron microscopy (SEM) (Philips XL 30, Eindhoven, The Netherlands) was performed at various magnifications under an acceleration voltage of 15 kV to observe the different groups' surface topography ($n = 1$ per group).

The second step was to determine the roughness parameters by optical interferometry (IFM) (Phase View 2.5, Palaiseau, France). Three implants of each surface were evaluated at the flat region of the implant cutting edges (three measurements per implant) and S_a (arithmetic average high deviation) and S_q (root mean square) parameters determined. A filter size of 250×250 μm^2 was utilized. Following data normality verification, statistical analysis at 95% level of significance was performed by one-way ANOVA.

The third procedure was the surface specific chemical assessment performed by x-ray photoelectron spectroscopy (XPS). The implants were inserted in a vacuum transfer chamber and degassed to 10^{-7} torr. The samples were then transferred under vacuum to a Kratos Axis 165 multitechnique XPS spectrometer (Kratos Analytical, Chestnut Ridge, NY). Survey spectra were obtained using a 165 mm mean radius concentric hemispherical analyzer operated at constant pass energy of 160 eV for survey and 80 eV for high resolution scans. The take off angle was 90° and a spot size of 150×150 μm^2 was used. The implant surfaces were evaluated at various locations (three per implant).

In vivo model and surgical procedure

The *in vivo* study comprised of 18 adult male beagles of ~1.5 years old. The study was approved by the Ethics Committee for Animal Research at the École Nationale Vétérinaire d'Alfort (Maisons-Alfort, Val-de-Marne, France). The beagles remained in the facility for 2 weeks prior to the surgical procedures.

For surgery, three drugs were administered until general anesthesia achievement by intramuscular injection. The drugs were atropine sulfate (0.044 mg/kg), xylazine chlorate (8 mg/kg), and ketamine chlorate (15 mg/kg). The implantation site was the radius epiphysis. Batches of six beagles were utilized for each evaluation time *in vivo*, where each animal received one implant of each group in each radii (one limb provided sample for biomechanical testing and the other for histologic evaluation).

For implant placement, the surgical site was shaved with a razor blade followed by application of antiseptic iodine solution. An incision of ~5 cm through the skin and periosteum was performed and the periosteum was elevated for bone exposure.

Sequential drills were utilized following the manufacturer's recommendation at 1200 rpm under abundant saline irrigation. The different implant groups were alternately placed from proximal to distal at distances of 1 cm from each other along the central region of the bone. The starting implant surface was also alternated between dogs to minimize bias in the torque and histomorphometric evaluation.

After placement the healing caps were inserted and sutured in layers with vicryl 4-0 (Ethicon Johnson, Miami, FL) for periosteum and nylon 4-0 (Ethicon Johnson, Miami, FL) for skin. The dogs stayed in animal care facility and received antibiotic (Benzyl Penicilin Benzatine 20.000 UI/Kg) and anti-inflammatory (Ketoprofen 1% 1 mL/5 kg) medication to control the pain and infection. Euthanasia was performed after 1, 3, and 6 weeks by anesthesia overdose and the limbs were retrieved by sharp dissection.

Torque testing was performed immediately after euthanization. The radius was adapted to an electronic torque machine equipped with a 500 Ncm torque load cell (Test Resources, Shakopee, MN). Custom machined tooling was adapted to each implant's internal connection and the bone block was carefully positioned to avoid specimen misalignment during testing. The implants were torqued in counter clockwise direction at a rate of ~0.196 radians/min and a torque versus displacement curve was recorded for each specimen.

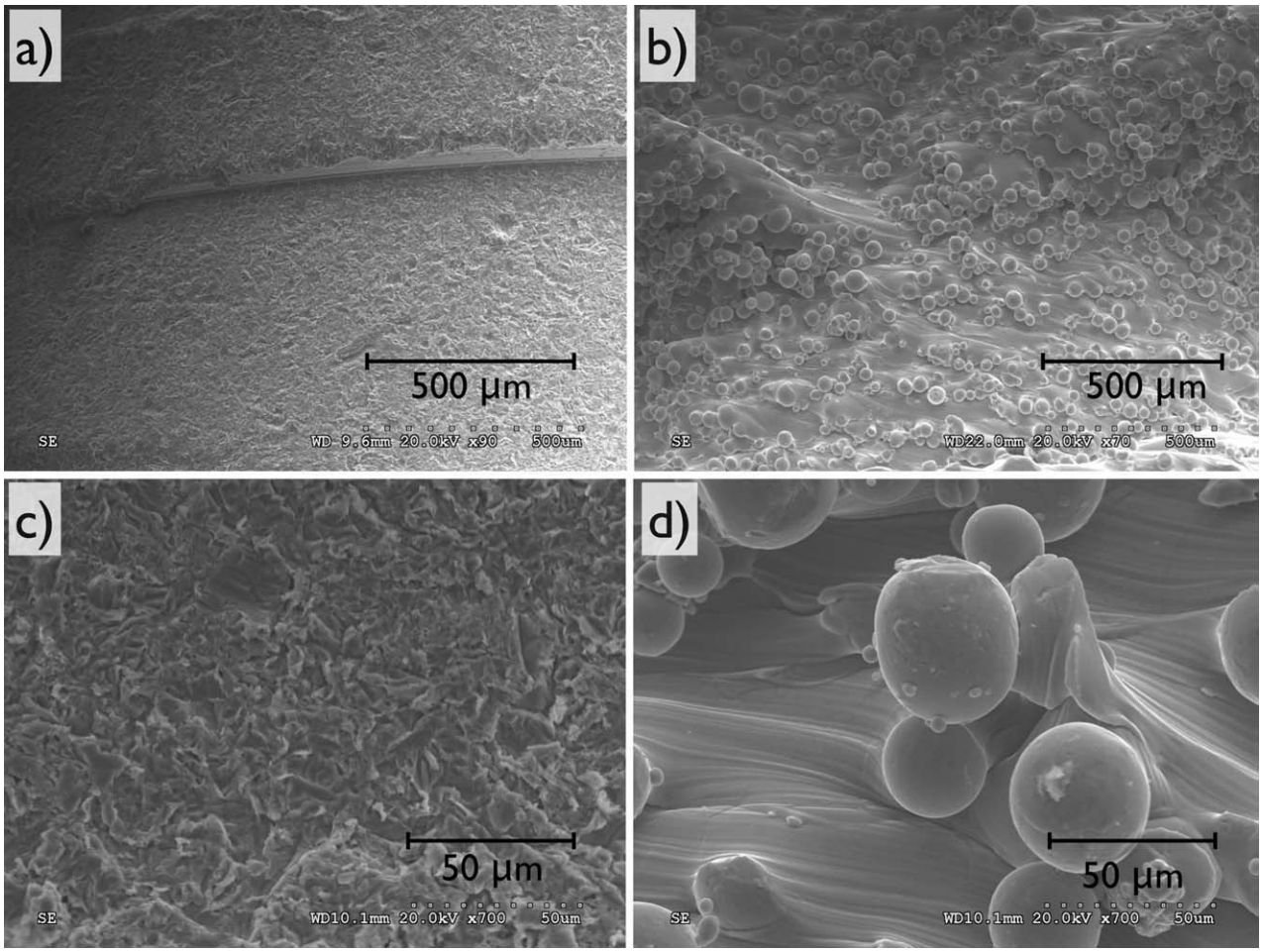

FIGURE 1. SEM of Alumina-Blasted/Acid-Etched (a and c) and Laser Sintered (b and d) presented different surface roughness morphology, which can be seen at low and high magnification.

Histomorphometric analysis

The implants in bone were reduced to blocks and immersed in 10% buffered formalin solution for 24 h. The blocks were then washed in running water for 24 h, and gradually dehydrated in a series of alcohol solutions ranging from 70 to 100% ethanol. Following dehydration, the samples were embedded in a methacrylate-based resin (Technovit 9100, Heraeus Kulzer GmbH, Wehrheim, Germany) according to the manufacturer's instructions. The blocks were then cut into slices (~300 µm thickness) aiming the center of the implant along its long axis with a precision diamond saw (Isomet 2000, Buehler, Lake Bluff), glued to acrylic plates with an acrylate-based cement, and a 24 h setting time was allowed prior to grinding and polishing. The sections were then reduced to a final thickness of ~30 µm by means of a series of SiC abrasive papers (400, 600, 800, 1200, and 2400) (Buehler, Lake Bluff, IL) in a grinding/polishing machine (Metaserv 3000, Buehler, Lake Bluff, IL) under water irrigation.[16] The sections were then toluidine blue stained and referred to optical microscopy for histomorphologic evaluation.

The bone-to-implant contact (BIC) was determined at 50× to 200× magnification (Leica DM2500M, Leica Microsystems GmbH, Wetzlar, Germany) by means of a computer software (Leica Application Suite, Leica Microsystems GmbH, Wetzlar, Germany). The regions of bone-to-implant contact along the implant perimeter were subtracted from the total implant perimeter, and calculations were performed to determine the BIC. The bone area fraction occupied (BAFO) between threads in trabecular bone regions was determined at 100× magnification (Leica DM2500M, Leica Microsystems GmbH, Wetzlar, Germany) by means of computer software (Leica Application Suite, Leica Microsystems GmbH, Wetzlar, Germany). The areas occupied by bone were subtracted from the total area between threads, and calculations were performed to determine the BAFO (reported in percentage values of bone area fraction occupied).[17]

Preliminary statistical analyses showed no effect of implant site (i.e., there were no consistent effects of positions 1 and 2 along the radius) on all measurements. Therefore, site was not considered further in the analysis. Statistical evaluation of torque, BIC, and BAFO was performed by Friedman's test. Statistical significance was indicated by *p*-levels less than 5%.

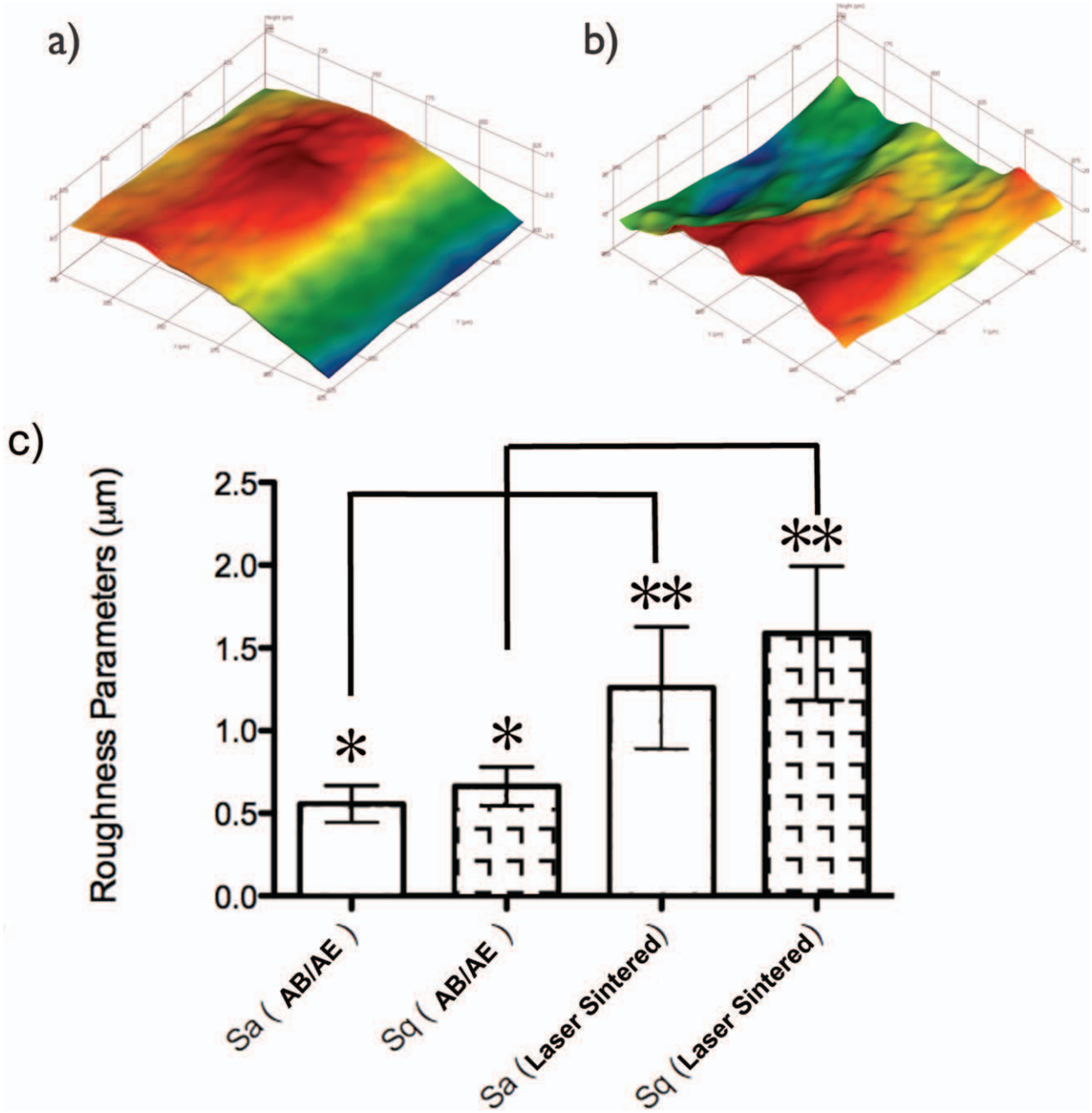

FIGURE 2. (a, b) Representative IFM reconstruction (filter size of 250 × 250 μm^2) of the AB/AE and laser sintered implants, respectively, (c) Bar graph (mean 95% CI) representing the surface roughness parameters, S_a and S_q also illustrating a significant difference, $p < 0.02$ (asterisks represent statistically homogenous groups. [Color figure can be viewed in the online issue, which is available at wileyonlinelibrary.com.]

RESULTS

Surface characterization

Implant surfaces' electron micrographs are presented in Figure 1 and their representative 250 μm × 250 μm IFM three-dimensional reconstructions, in Figure 2(A,B). Their respective S_a and S_q values are presented in Figure 2(C,D). The surface texture observed at intermediate and high magnification levels (Figure 1), as well as the IFM

TABLE I. X-Ray Photoelectron Spectroscopy Atomic Percentages for the AB/AE and Laser Sintered Implants

	Al2p	C1s	O1s	Ti2p	V2p3
AB/AE	3.43 (1.2)	31.82 (4.2)	45.3 (3.3)	13.21 (2.2)	0.43 (0.15)
Laser sintered	2.88 (0.9)	42.1 (3.8)	35.09 (2.8)	10.64 (3.2)	0.21 (0.11)

Mean (± SD).

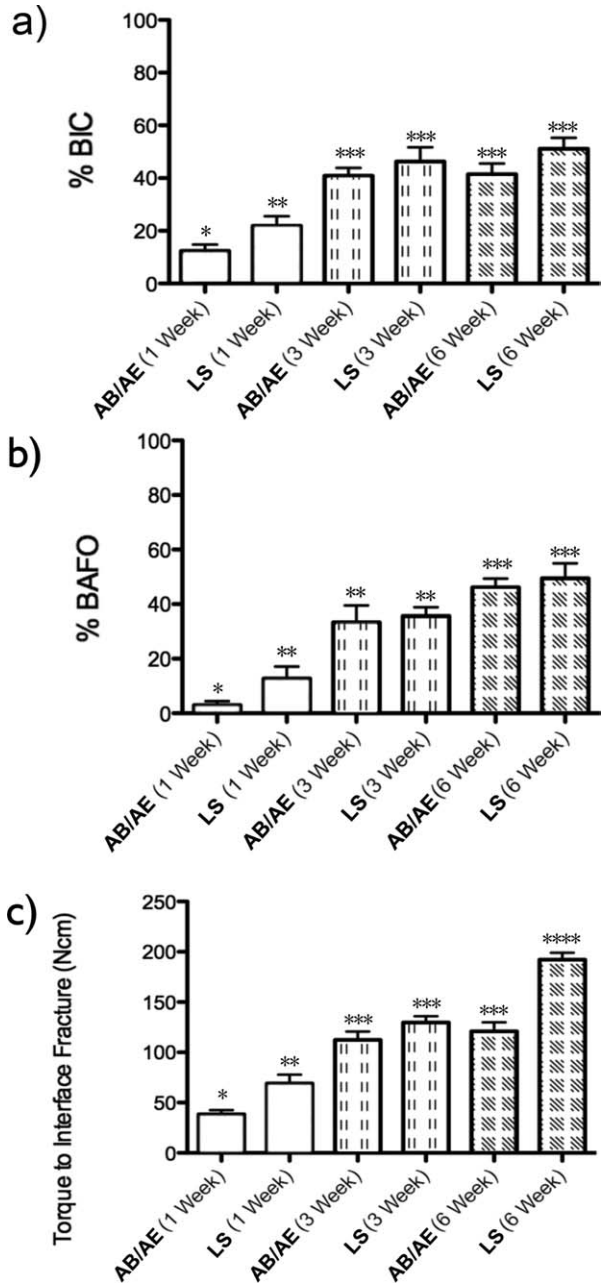

FIGURE 3. (a) Bone-to-implant contact ($p < 0.02$). (b) Bone area fraction occupancy ($p < 0.02$), and (c) Torque to interface failure ($p < 0.01$) statistics summary (mean ± 95% CI) for the different implants and times *in vivo* (asterisks represent statically homogenous groups).

reconstruction [Figure 2(A,B)] revealed morphologic differences between the two groups. The IFM measurements presented significant differences for both S_a and S_q values [Figure 2(C)], where the experimental (laser sintered) implant presented the higher values. Mean S_a and S_q values were 0.56 μm (0.11 μm, 95% CI) and 0.66 μm (0.11 μm, 95% CI) for AB/AE and 1.26 μm and 1.59 μm for Laser Sintered, respectively (0.35 μm and 0.38 μm, 95 % CI).

The XPS spectra demonstrated the presence of Al, C, O, Ti, and V for the different surfaces (Table I). The highest aluminum concentration was observed for the AB/AE likely due to the alumina blasting procedure. Higher O, Ti, and V concentrations were observed for the AB/AE surface. Conversely, higher C values were detected for the experimental (laser sintered) surface (Table I).

In vivo model

The animal surgical procedures and follow-up demonstrated no complications regarding procedural conditions, postoperative infection, or other clinical concerns. No implants were excluded from the study due to clinical instability immediately after the euthanization.

The biomechanical testing showed that significantly higher torque to interface fracture was observed for the experimental surface relative to control at 1 week ($p = 0.011$), but that at 3 weeks no differences were observed between surfaces ($p = 0.129$). At 6 weeks, a significantly higher removal torque ($p < 0.002$) was observed for the experimental surface in comparison to the control (Figure 3).

The nondecalcified sample processing showed intimate bone contact with all implant surfaces at regions of cortical and trabecular bone (Figure 4). Qualitative evaluation of the toluidine blue stained thin sections revealed no morphologic differences between surfaces at 1 and 3 weeks *in vivo,* where intimate contact between cortical and trabecular bone was observed. In addition, different healing patterns were observed at specific regions along the implant bulk, depending on the interplay between device geometry and surgical instrumentation dimensions (Figure 4).

At the region of the implant where the inner thread diameter was larger or equal the final surgical drilling dimension allowing intimate contact between implant surface and cortical bone immediately after implantation, substantial bone remodeling in proximity with the implant surface occurred between 1 [Figure 4(A,D)] and 3 [Figure 4(B,E)] weeks *in vivo* for all groups. While at 1 week *in vivo* old bone remodeling was observed along with regions of newly formed woven bone [Figure 4(A,D)], at 3 weeks substantial woven bone was observed in proximity with the implant surface [Figure 4(B,E)].

At regions where a healing chamber was formed due to the formation of a space between the outer diameter of the surgical instrumentation and the inner diameter of the implant, woven bone formation was observed throughout the space of the chamber and directly onto the implant surface at 3 weeks *in vivo* [Figure 4(B,E)]. At 6 weeks, woven bone replacement by lamellar bone was observed throughout the healing chamber [Figure 4(C,D)] in both groups.

At trabecular bone regions, newly formed woven bone was observed at 3 weeks [Figure 4(B,E)], and its replacement by lamellar bone was observed at 6 weeks [Figure 4(C,F)] at regions in proximity with all implant surfaces.

The histomorphometric results demonstrated a significant difference between experimental groups for BIC at 1 week *in vivo* ($p < 0.04$) with the laser sintered having a higher value, whereas the 3 and 6 weeks *in vivo* exhibited no significant differences between groups [$p > 0.40$ and $p > 0.11$, respectively – Figure 3(A)]. The same trend was observed for BAFO, where a significant difference was

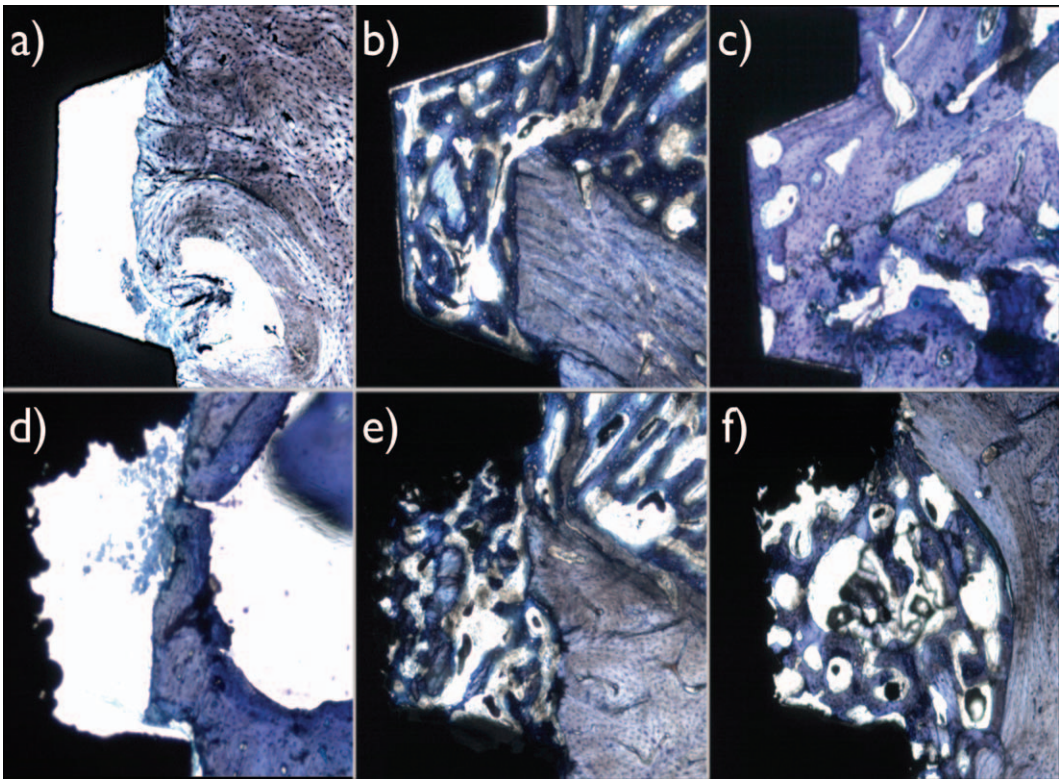

FIGURE 4. Optical micrographs at the top depicting 1, 3, and 6 weeks observation period for AB/AE implant surface (a, b, and c) and the same time points at the bottom for laser sintered (d, e, and f). [Color figure can be viewed in the online issue, which is available at wileyonlinelibrary.com.]

observed at 1 week (significantly higher for laser sintered, $p < 0.03$), but not at 3, and 6 weeks *in vivo* [$p > 0.70$. and $p > 0.60$, respectively—Figure 3(B)].

DISCUSSION

Both histomorphometric parameters evaluated in this study were significantly higher for the laser sintered compared with the AB/AE only in the first week evaluation with values being not significantly different at the subsequent observation periods (3 and 6 weeks *in vivo*). As per the imaging results, the three-dimensional surface configuration of the laser sintered implant may have provided larger surface area during the early stages of wound healing with increased blood clot retention compared to the AB/AE. General BIC and BAFO measurements were in agreement with the biomechanical results, where torque was significantly higher for the laser sintered at 1 week and then not significantly different to the AB/AE at 3 weeks. At 6 weeks when more time was allowed for early bone healing, the histomorphometric results remained not significantly different between groups whereas significantly higher torque was observed for the experimental relative to the control implant group. The 6 weeks results for BIC and BAFO contrasting with torque-to-interface failure test is in agreement with the claim that static osseointegration histomorphometric parameters may fail to represent the bone/implant interface mechanical properties. From a clinical standpoint, lower BIC and BAFO may be preferred on a higher mechanical property bone implant interface compared with a higher BIC and BAFO on a lower mechanical property bone that may yield reduced stability.[1]

The implant surface physical characterization showed that both arithmetic mean of the absolute values of the surface height within the sampling area and the root mean square of the surface departures were significantly higher for the laser sintered relative to AB/AE surface. It is possible that the observed 1 week significantly higher torque for the laser sintered relative to the AB/AE is likely a function of the higher resistance to torque provided by the increased surface texture of the former, and should not be suggestive as a motivation for immediate loading since the following observation period (3 weeks) revealed no statistical difference in torque between groups. At early observation periods, such as 1 week, torque resistance seems to be highly influenced by surface topography since osseointegration process is at its very initial stage.[18] The similar results obtained at 3 weeks may be elucidated by the described early bone healing events shown for screw-root form implants with healing chambers where intense bone remodeling and resorption is observed at the regions where the interplay between surgical techniques and implant macrodesign allows an intimate contact between bone and implant.[17,19–22] Because at 3 week woven bone was under formation at healing chamber regions and bone resorption was occurring at the implant outer threads, torque levels were similar irrespective of implant group. However, with initial lamellar bone formation in the healing chamber region, the significant increase in torque values at 6 week

for the laser sintered suggests that the surface topography was an important factor for improved bone response. The S_a mean value (1.26 μm) for the laser sintered fell within the moderately rough range, shown to provide the strongest bone response compared to minimally rough (S_a 0.5–1 μm) surfaces such as the AB/AE (0.56 μm).[23]

From a temporal standpoint, both topographic and chemistry surface modifications have drawn attention,[1,5,6,24,25] as both have been showing promising results *in vitro*[26] and *in vivo*[27–35] relative to their moderately rough predecessors. As for implant physical modifications at the nanometric scale, the resulting surface configuration that can be tailored on a laser sintered implant for improved bone response is yet to be understood. Several processing parameters seem to have an effect on the final surface topography of laser sintered implants and likely on its osseoconductive properties, such as the power rating of the laser, the diameter of the laser beam focus, the scanning speed, the average particle size of the starting material powder, the process atmospheric conditions and others.[36] Nonetheless, our surface chemistry results are suggestive that only biocompatible elements along with adsorbed carbon species were present at the surface indicating that the fabrication technique was suitable for biomedical applications. Therefore, future investigation with variations in such processing parameters along with surface physico-chemical characterization and *in vivo* experimentation is warranted.

An *in vitro* study comparing acid-etched and laser sintered titanium surfaces has shown improved osteoblastic differentiation, production of bone morphogenetic protein, vascular endothelial growth factor and specific bone proteins for the laser sintered likely due to the controlled porous topography.[37] Although a clinical short-term comparison of AB/AE and laser sintered microimplants have reported significantly higher bone density in the threaded area for the laser sintered surface, no differences in BIC or in bone density outside the threaded area measurements were detected.[38] Therefore, several temporal evaluations became key to understanding the potential differences in healing events between different surfaces.

Although several animal models, such as the rabbit, pig, sheep, goat, and others could suit *in vivo* research, the canine model has shown close similarity in bone composition to that of human,[39] and has been indicated as one of the most appropriate for the testing of implant materials.[40] Differences in remodeling rate must be acknowledged and have been reported for example between the canine model and human.[41]

Our postulated hypothesis that laser sintered implants would improve early biomechanical and histomorphometric parameters compared to an AB/AE implant surface was partially accepted, since only higher torque to interface failure was observed at 1 and 6 week, but no differences were found for BIC and BAFO.

REFERENCES

1. Coelho PG, Granjeiro JM, Romanos GE, Suzuki M, Silva NR, Cardaropoli G, Thompson VP, Lemons JE. Basic research methods and current trends of dental implant surfaces. J Biomed Mater Res B Appl Biomater 2009;88:579–596.
2. Jimbo R, Ono D, Hirakawa Y, Odatsu T, Tanaka T, Sawase T. Accelerated photo-induced hydrophilicity promotes osseointegration: An animal study. Clin Implant Dent Relat Res 2011;13:79–85.
3. Jimbo R, Sawase T, Baba K, Kurogi T, Shibata Y, Atsuta M. Enhanced initial cell responses to chemically modified anodized titanium. Clin Implant Dent Relat Res 2008;10:55–61.
4. Albrektsson T, Gottlow J, Meirelles L, Ostman PO, Rocci A, Sennerby L. Survival of NobelDirect implants: An analysis of 550 consecutively placed implants at 18 different clinical centers. Clin Implant Dent Relat Res 2007;9:65–70.
5. Albrektsson T, Wennerberg A. Oral implant surfaces. I. Review focusing on topographic and chemical properties of different surfaces and in vivo responses to them. Int J Prosthodont 2004;17: 536–543.
6. Albrektsson T, Wennerberg A. Oral implant surfaces. II. Review focusing on clinical knowledge of different surfaces. Int J Prosthodont 2004;17:544–564.
7. Jimbo R, Sawase T, Shibata Y, Hirata K, Hishikawa Y, Tanaka Y, Bessho K, Ikeda T, Atsuta M. Enhanced osseointegration by the chemotactic activity of plasma fibronectin for cellular fibronectin positive cells. Biomaterials 2007;28:3469–3477.
8. Wennerberg A, Albrektsson T. On implant surfaces: A review of current knowledge and opinions. Int J Oral Maxillofac Implants 2010;25:63–74.
9. Mangano C, Piattelli A, Raspanti M, Mangano F, Cassoni A, Iezzi G, Shibli JA. Scanning electron microscopy (SEM) and X-ray dispersive spectrometry evaluation of direct laser metal sintering surface and human bone interface: A case series. Las Med Sci 2011;26:133–138.
10. Lopez-Heredia MA, Sohier J, Gaillard C, Quillard S, Dorget M, Layrolle P. Rapid prototyped porous titanium coated with calcium phosphate as a scaffold for bone tissue engineering. Biomaterials 2008;29:2608–2615.
11. Traini T, Mangano C, Sammons RL, Mangano F, Macchi A, Piattelli A. Direct laser metal sintering as a new approach to fabrication of an isoelastic functionally graded material for manufacture of porous titanium dental implants. Dent Mater 2008;24: 1525–1533.
12. Xue W, Krishna BV, Bandyopadhyay A, Bose S. Processing and biocompatibility evaluation of laser processed porous titanium. Acta Biomater 2007;3:1007–1018.
13. Li JP, de Wijn JR, Van Blitterswijk CA, de Groot K. Porous Ti6Al4V scaffold directly fabricating by rapid prototyping: preparation and in vitro experiment. Biomaterials 2006;27:1223–1235.
14. Bertol LS, Júnior WK, Silva FP, Aumund-Kopp C. Medical design: Direct metal laser sintering of Ti-6Al-4V. Mater Des 2010;31: 3982–3988.
15. Mangano C, Mangano F, Shibli JA, Luongo G, De Franco M, Briguglio F, Figliuzzi M, Eccellente T, Rapani C, Piombino M, Macchi A. Prospective clinical evaluation of 201 direct laser metal forming implants: Results from a 1-year multicenter study. Las Med Sci 2012;27:181–189.
16. Donath K, Breuner G. A method for the study of undecalcified bones and teeth with attached soft tissues. The Sage-Schliff (sawing and grinding) technique. J Oral Pathol 1982;11:318–326.
17. Leonard G, Coelho P, Polyzois I, Stassen L, Claffey N. A study of the bone healing kinetics of plateau versus screw root design titanium dental implants. Clin Oral Implants Res 2009;20:232–239.
18. Löberg J, Mattisson I, Hansson S, Ahlberg E. Characterisation of titanium dental implants i: Critical assessment of surface roughness parameters. Open Biomater J 2010;2:18–35.
19. Berglundh T, Abrahamsson I, Lang NP, Lindhe J. De novo alveolar bone formation adjacent to endosseous implants. Clin Oral Implants Res 2003;14:251–262.
20. Bonfante EA, Granato R, Marin C, Suzuki M, Oliveira SR, Giro G, Coelho PG. Early bone healing and biomechanical fixation of dual acid-etched and as-machined implants with healing chambers: An experimental study in dogs. Int J Oral Maxillofac Implants 2011; 26:75–82.
21. Coelho PG, Suzuki M, Guimaraes MV, Marin C, Granato R, Gil JN, Miller RJ. Early bone healing around different implant bulk

designs and surgical techniques: A study in dogs. Clin Implant Dent Relat Res 2010;12:202–208.
22. Marin C, Granato R, Suzuki M, Gil JN, Janal MN, Coelho PG. Histomorphologic and histomorphometric evaluation of various endosseous implant healing chamber configurations at early implantation times: A study in dogs. Clin Oral Implants Res 2010;21: 577–583.
23. Wennerberg A, Albrektsson T. Effects of titanium surface topography on bone integration: A systematic review. Clin Oral Implants Res 2009;20(Suppl 4):172–184.
24. Kang BS, Sul YT, Oh SJ, Lee HJ, Albrektsson T. XPS, AES and SEM analysis of recent dental implants. Acta Biomater 2009;5: 2222–2229.
25. Dohan Ehrenfest DM, Coelho PG, Kang BS, Sul YT, Albrektsson T. Classification of osseointegrated implant surfaces: Materials, chemistry and topography. Trends Biotechnol 2010;28:198–206.
26. Moura CC, Souza MA, Dechichi P, Zanetta-Barbosa D, Teixeira CC, Coelho PG. The effect of a nanothickness coating on rough titanium substrate in the osteogenic properties of human bone cells. J Biomed Mater Res A 2010;94:103–111.
27. Coelho PG, Cardaropoli G, Suzuki M, Lemons JE. Early healing of nanothickness bioceramic coatings on dental implants. An experimental study in dogs. J Biomed Mater Res B Appl Biomater 2009; 88:387–393.
28. Coelho PG, Lemons JE. Physico/chemical characterization and in vivo evaluation of nanothickness bioceramic depositions on alumina-blasted/acid-etched Ti-6Al-4V implant surfaces. J Biomed Mater Res A 2009;90:351–361.
29. Coelho PG, Marin C, Granato R, Suzuki M. Clinical device-related article: Histomorphologic analysis of 30 plateau root form implants retrieved after 8 to 13 years in function. A human retrieval study. J Biomed Mater Res B Appl Biomater 2009;91: 975–979.
30. Coelho PG, Suzuki M, Guimaraes MV, Marin C, Granato R, Gil JN, Miller RJ. Early bone healing around different implant bulk designs and surgical techniques: A study in dogs. Clin Implant Dent Relat Res 2010;12:202–208.
31. Granato R, Marin C, Suzuki M, Gil JN, Janal MN, Coelho PG. Biomechanical and histomorphometric evaluation of a thin ion beam bioceramic deposition on plateau root form implants: An experimental study in dogs. J Biomed Mater Res B Appl Biomater 2009;90:396–403.
32. Granato R, Marin C, Suzuki M, Gil JN, Janal MN, Coelho PG. Biomechanical and histomorphometric evaluation of a thin ion beam bioceramic deposition on plateau root form implants: an experimental study in dogs. J Biomed Mater Res B Appl Biomater 2009; 90:396–403.
33. Marin C, Granato R, Suzuki M, Gil JN, Piattelli A, Coelho PG. Removal torque and histomorphometric evaluation of bioceramic grit-blasted/acid-etched and dual acid-etched implant surfaces: An experimental study in dogs. J Periodontol 2008;79:1942–1949.
34. Mendes VC, Moineddin R, Davies JE. The effect of discrete calcium phosphate nanocrystals on bone-bonding to titanium surfaces. Biomaterials 2007;28:4748–4755.
35. Mendes VC, Moineddin R, Davies JE. Discrete calcium phosphate nanocrystalline deposition enhances osteoconduction on titanium-based implant surfaces. J Biomed Mater Res A 2009;90: 577–585.
36. Hollander DA, von Walter M, Wirtz T, Sellei R, Schmidt-Rohlfing B, Paar O, Erli HJ. Structural, mechanical and in vitro characterization of individually structured Ti-6Al-4V produced by direct laser forming. Biomaterials 2006;27:955–963.
37. Mangano C, De Rosa A, Desiderio V, d'Aquino R, Piattelli A, De Francesco F, Tirino V, Mangano F, Papaccio G. The osteoblastic differentiation of dental pulp stem cells and bone formation on different titanium surface textures. Biomaterials 2010;31:3543–3551.
38. Shibli JA, Mangano C, D'Avila S, Piattelli A, Pecora GE, Mangano F, Onuma T, Cardoso LA, Ferrari DS, Aguiar KC, et al. Influence of direct laser fabrication implant topography on type IV bone: A histomorphometric study in humans. J Biomed Mater Res A 2010;93:607–614.
39. Aerssens J, Boonen S, Lowet G, Dequeker J. Interspecies differences in bone composition, density, and quality: Potential implications for in vivo bone research. Endocrinol 1998;139:663–670.
40. Pearce AI, Richards RG, Milz S, Schneider E, Pearce SG. Animal models for implant biomaterial research in bone: A review. Eur Cells Mater 2007;13:1–10.
41. Bloebaum RD, Ota DT, Skedros JG, Mantas JP. Comparison of human and canine external femoral morphologies in the context of total hip replacement. J Biomed Mater Res 1993;27:1149–1159.